in which the soil is more compacted or areas in which there are boulders or outcroppings of rock that are not blanketed by dust. In the absence of images of the regions of Mercury observed by the radiometer, we cannot comment on possible relationships between the thermal structure and surface morphology.

S. C. CHASE
Santa Barbara Research Center, Goleta, California 93017
E. D. MINER
Jet Propulsion Laboratory, California Institute of Technology, Pasadena 91103
D. MORRISON
Institute for Astronomy, University of Hawaii, Honolulu 96822
G. MÜNCH
G. NEUGEBAUER, M. SCHROEDER
California Institute of Technology, Pasadena 91109

References and Notes

1. The thermal inertia is the square root of the product of the thermal conductivity (K) and the heat capacity per unit volume (ρc). In this report we express this parameter in the familiar units of cal cm^{-2} sec$^{-1/2}$ °K^{-1}; these numbers can be converted to S.I. units of erg cm^{-2} sec$^{-1/2}$ °K^{-1} by multiplying by 4.2×10^7 erg/cal.
2. S. C. Chase, *Appl. Opt.* **8**, 639 (1969).
3. The maximum temperature expected, near noon on the equator, was 560°K at the time of the Mariner 10 encounter. The substantial variations in the maximum temperatures with hermographic longitude that result from the high eccentricity of the orbit of Mercury are not expected to affect the nighttime temperatures significantly.
4. The models assume a homogeneous material with temperature-independent thermal properties and a plane-parallel geometry. The method of calculation is described by D. Morrison [*Smithson. Astrophys. Obs. Spec. Rep. No. 292* (1969) and (*5*)]. As shown in these references, the existence of temperature-dependent thermal properties has little effect on calculated surface temperatures.
5. D. Morrison, *Space Sci. Rev.* **11**, 271 (1970).
6. For a general review of Earth-based studies of the thermophysics of Mercury, see Morrison (*5*).
7. E. Pettit and S. B. Nicholson, *Publ. Astron. Soc. Pac.* **35**, 194 (1923). For additional discussion see Soter (*8*) and Morrison (*5*).
8. S. L. Soter, *Science* **153**, 1112 (1966).
9. B. C. Murray, *Trans. Am. Geophys. Union* **48**, 148 (1967).
10. T. L. Murdock and E. P. Ney, *Science* **170**, 535 (1970).
11. The ratio of skin depths is determined primarily by the observations at 3.3 mm by E. E. Epstein, M. M. Dworetsky, W. G. Fogarty, J. W. Montgomery, and R. C. Cooley [*Radio Sci.* **5**, 401 (1970)] and at 3.75 cm by M. J. Klein (*ibid.*, p. 397). More recent microwave measurements are reported in D. Morrison and M. J. Klein, *Astrophys. J.* **160**, 325 (1970); B. L. Ulich, J. R. Cogdell, J. H. Davis, *Icarus* **19**, 59 (1973); F. H. Briggs and F. D. Drake, *Astrophys. J.* **182**, 601 (1973); and J. N. Cuzzi, *ibid.*, in press.
12. M. J. Campbell and J. Ulrichs, *J. Geophys. Res.* **74**, 5867 (1969).
13. We thank the entire Mariner team, both at Jet Propulsion Laboratory and at Santa Barbara Research Center, for making the mission successful. We thank J. Bennett for help with the data analysis, J. Engel for his work as leader of the radiometry group at SBRC, and T. Clarke for his work as instrument engineer.

31 May 1974

Observations at Mercury Encounter by the Plasma Science Experiment on Mariner 10

Abstract. *A fully developed bow shock and magnetosheath were observed near Mercury, providing unambiguous evidence for a strong interaction between Mercury and the solar wind. Inside the sheath there is a distinct region analogous to the magnetosphere or magnetotail of Earth, populated by electrons with lower density and higher temperature than the electrons observed in the solar wind or magnetosheath. At the time of encounter, conditions were such that a perpendicular shock was observed on the inbound leg and a parallel shock was observed on the outbound leg of the trajectory, and energetic plasma electron events were detected upstream from the outbound shock crossing. The interaction is most likely not atmospheric, but the data clearly indicate that the obstacle to solar wind flow is magnetic, either intrinsic or induced. The particle fluxes and energy spectra showed large variations while the spacecraft was inside the magnetosphere, and these variations could be either spatial or temporal.*

An unexpectedly strong interaction between the solar wind and Mercury was detected by the plasma science experiment (PSE) when Mariner 10 encountered Mercury on 29 March 1974. Before this encounter, the interaction was generally thought to resemble that of the moon, where the solar wind impinges directly on the surface. Planets, such as Earth and Jupiter, having strong magnetic fields, hold the solar wind off from the surface and deflect its flow around a cavity larger than the planet itself. Results from Mariner 5 and Mariner 10 have indicated that at Venus the solar wind is deflected by a well-developed ionosphere. Mercury presents to the solar wind an obstacle more analogous to Earth than to the moon or Venus.

This report presents preliminary results from the rearward-looking (antisolar) electrostatic analyzer which forms part of the plasma science experiment on Mariner 10. This experiment, a cooperative effort by groups from the Massachusetts Institute of Technology (MIT), the Los Alamos Scientific Laboratory (LASL), the Goddard Space Flight Center, and the University of California at Los Angeles, has been described previously (*1*) in connection with the encounter of Mariner 10 with Venus. These first measurements of plasma electrons in the vicinity of Mercury clearly show the presence of a bow shock and sheath region, resulting from deflection of the solar wind around the planet, enclosing a region which we tentatively identify as a "magnetosphere," containing a population of electrons whose properties differ from those in the surrounding medium, even though we cannot conclude whether they are trapped.

The data on which this interpretation

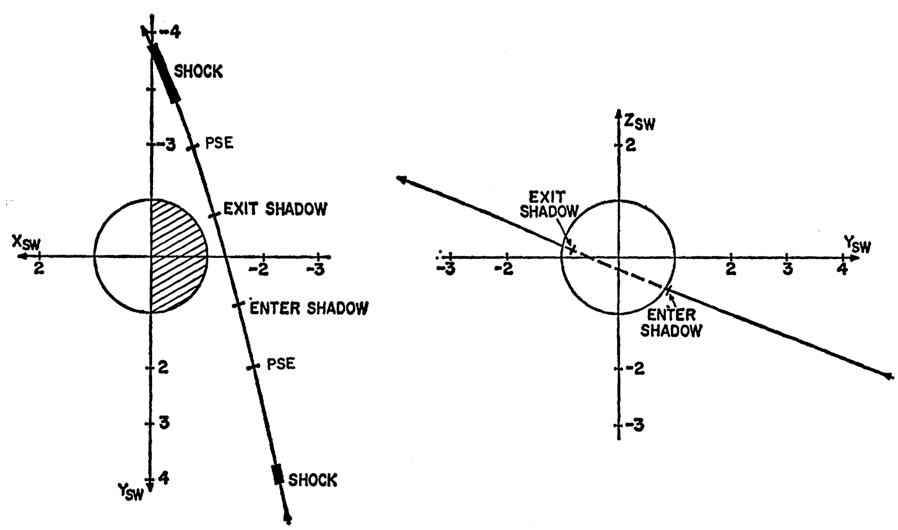

Fig. 1. The trajectory of Mariner 10 at the time of encounter with Mercury. Distances are in planetary radii, and the X_{sw} axis points in the antisolar wind direction taken to be 3° to the west of the sun. The Z_{sw} axis is to the north in the right-hand coordinate system.

is based consist of measurements of electron spectra taken every 6 seconds throughout the period of encounter. Each spectrum is composed of 15 differential flux measurements, each made in 0.4 second; the energy channels are logarithmically spaced between 13.4 and 687 ev with a fractional width in energy of 6.6 percent. The fan-shaped field of view of the instrument scans at a rate of 1° per second through an arc of 120° centered on a direction in the ecliptic plane 6.5° east of the spacecraft-sun line. The field of view is ± 3.5° in the scan plane and ± 13.5° perpendicular to that plane. The spacecraft passed on the dark side of the planet, along a trajectory shown in Fig. 1.

Prior to the encounter, the instrument measured typical interplanetary solar wind electron spectra, illustrated by spectrum 1 of Fig. 2. The spectra were similar in form to those taken near 1 A.U. (astronomical unit) having separate low-energy ("core") and high-energy ("halo") components which were both approximately Maxwellian in form and characterized by temperatures of 1.5×10^5 °K and 6×10^5 °K, respectively (*2*).

Figure 3 shows fluxes at 13.4, 71, and 389 ev and the electron density and pressure as a function of time for the period between 2000 and 2200 U.T. Earth-received time (ERT). A scale with the events referred to the time of closest approach is given at the bottom of Fig. 3, and the U.T. of spacecraft observation is given across the top. The density n and pressure P are defined in terms of the velocity distribution function, f, as follows:

$$n = \frac{4\pi}{\Delta\Omega} \int f \, d\bar{v}$$

$$P = 2\pi \frac{m}{\Delta\Omega} \int f \bar{v}^2 \, d\bar{v}$$

where $\Delta\Omega$ is the solid angle of acceptance of the detector; the integrations have been carried out numerically over the whole energy range of the detector, and extrapolation from 13.4 ev to zero has been made assuming a Maxwellian form for the distribution function. Modulation of the derived density and pressure by the solar wind flow velocity has not been removed; this modulation is less pronounced after encounter than before because of increased magnetic activity. The peak values of the scan modulation of the density and pressure are the most representative of ambient conditions.

From the variation with scan angle

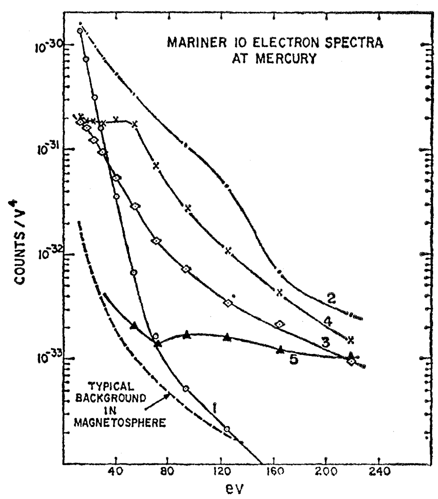

Fig. 2. Electron spectra at various times, given in the text, during the encounter. Spectrum 1 was taken in the interplanetary medium before the spacecraft reached the bow shock; spectrum 2 was taken in the magnetosheath; spectra 3 and 4 were taken in the magnetosphere; and spectrum 5 was taken between energetic particle events B and C, just before the spacecraft reentered the magnetosheath. A typical background as observed in the magnetosphere is shown; the background in the interplanetary medium is several times lower.

of electron flux at 13.4 ev at a time some 20 minutes before the spacecraft encountered the bow shock, we have determined a solar wind velocity of 630 ± 40 km sec^{-1}, and a mean flow direction in a frame moving with the planet of $3 \pm 6°$ from the west of the sun. The results of the MIT plasma experiments on Explorer 47 and Explorer 50 at 1 A.U. indicate bulk speeds, corrected for propagation and corotation, which corroborate this value. The preencounter conditions are $n = 17 \pm 2$ cm^{-3} and a ram pressure $\rho v^2 = 1.1 \times 10^{-7}$ dyne cm^{-2}.

We now describe the events illustrated in Fig. 3. On the incoming leg of the trajectory, the bow shock was traversed three times within 1 minute, beginning at −19 minutes, 38 ± 6 seconds and ending at −18 minutes, 49 ± 6 seconds, in agreement with the corresponding magnetometer observations (*3*) to within the resolution of the electron spectrometer. This thin shock structure closely resembles Earth's bow shock observed by an electron detector when the interplanetary magnetic field is approximately perpendicular to the direction of the shock normal ("perpendicular" shock) (*2*). Across the discontinuity there was a density change of approximately two times and a temperature change of approximately three times, in satisfactory agreement with observations of density and temperature jumps by electron detectors that have traversed Earth's bow shock at comparable locations (*2*).

After the shock traversals, we observed a region analogous to Earth's magnetosheath, where the flux of electrons at, for example, 71 ev, was greatly increased. Spectrum 2 of Fig. 2, taken in this region, does not show the "flat" form at low energies characteristic of electron spectra taken in Earth's magnetosheath (*2*) but does show the large increase of electron flux at moderate energies resulting from "thermalization" behind the shock. In the inner sheath, traversed between −17 and −13 minutes, there was a reduction in flux above about 100 ev which varied with the direction of pointing of the detector. The observations made during that period will be discussed below.

At −10 minutes there was a well-defined change in spectral form (from that shown in Fig. 2 as spectrum 2 to that shown as spectrum 3), accompanied by a drop in density to about 1 cm^{-3}. There was an abrupt increase in electron flux between 200 and 680 ev at this time. Comparing these plasma data with similar observations made near Earth (*4*), we conclude that the spacecraft crossed a boundary analogous to a magnetopause. This interpretation is strengthened by changes in the magnetic field observed at the same time (*3*). Fluctuations in the data limit the accuracy with which the time of crossing can be determined to about 1 minute.

The spacecraft passed into the optical shadow of the planet at −4 minutes, 48 seconds, after which the electron spectra gradually assumed the form of spectrum 4 in Fig. 2, as a result of increasing electron fluxes at all energies. Passage out of the shadow of the planet occurred at +2 minutes, 39 seconds.

A second traversal of the magnetopause boundary occurred at approximately +7 minutes when the density and spectral form became similar to those observed immediately after the shock crossing on the inbound leg of the trajectory. Between +12 and +17 minutes the spacecraft passed through a highly disturbed region, which we interpret as a pulsating ("parallel") shock (*5*). This interpretation is consistent with the nature of the incoming shock, the geometry of the orbit and shock boundary, and the measured direction of the magnetic field before and after the encounter (*3*). In this region the plasma properties varied rapidly with time, and it is possible that at least some of the electron spectra are inaccurate because of possible large fluctuations during a single measurement sequence. After this shock passage, typical solar wind spectra and fluid parameters were observed; in addition, "upstream events" were seen as indicated in Fig. 3. These events are qualitatively similar to those recorded by electron detectors situated upstream of Earth's bow shock on magnetic field lines intersecting the bow shock (*6*). Increases in the 71-ev flux before encounter (for example, at −26 minutes) appear to be different in nature from those observed after encounter; the former coincide with transient decreases in the interplanetary magnetic field (*3*). The presence of upstream events is consistent with our interpretation of the outgoing shock as having parallel geometry. We show in Fig. 4 a comparison between the observations presented here and observations of a parallel shock at Earth made by the triaxial electron spectrometer on Orbiting Geophysical Observatory, OGO-5, which had a time response similar to that of the instrument used here. The times scale according to which the Mercury data have been plotted has been adjusted by the ratio $[c/(\omega_{pe}\ V_{se})_{Earth}]/[c/(\omega_{pe}\ V_{se})_{Mercury}]$ to take account of plasma conditions and the speed of the observer, V_{se}, where c is the speed of light and ω_{pe} is the electron plasma frequency. The similarity between observations at Mercury and Earth is quite striking.

At the times marked on Fig. 3 by the letters A, B, C, and D, the University of Chicago energetic particle experiment (*7*) recorded high-intensity bursts of energetic electrons of short duration. During bursts B and C, energetic protons were also identified. The response of the plasma instrument showed no change in flux or in spectral shape during events A and D. Changes in these quantities did take place during events B and C. After event A, the spectrum was similar to spectrum 4 of Fig. 2. Shortly after event B began (at +1 minute, 31 seconds), the counting rates in our intermediate energy channels fell to the background value, leaving only low rates in the energy channels below 20 ev and in channels above 389 ev. The spectrum then relaxed to the form shown as spectrum 5 in Fig. 2, and retained this shape and approximately the same intensity until +6 minutes, 43 seconds in the middle of event C. After this there were two spectra in which the counting rates at intermediate energies were again reduced to their background values. Then the spacecraft entered the magnetosheath, and the spectrum returned to the form of spectrum 2 of Fig. 2.

Having described the major features of the observations, we now consider features of particular interest in more detail and interpret them in terms of the interaction of Mercury with the solar wind. First, let us consider the possibility that the interaction is with a neutral atmosphere or with an iono-

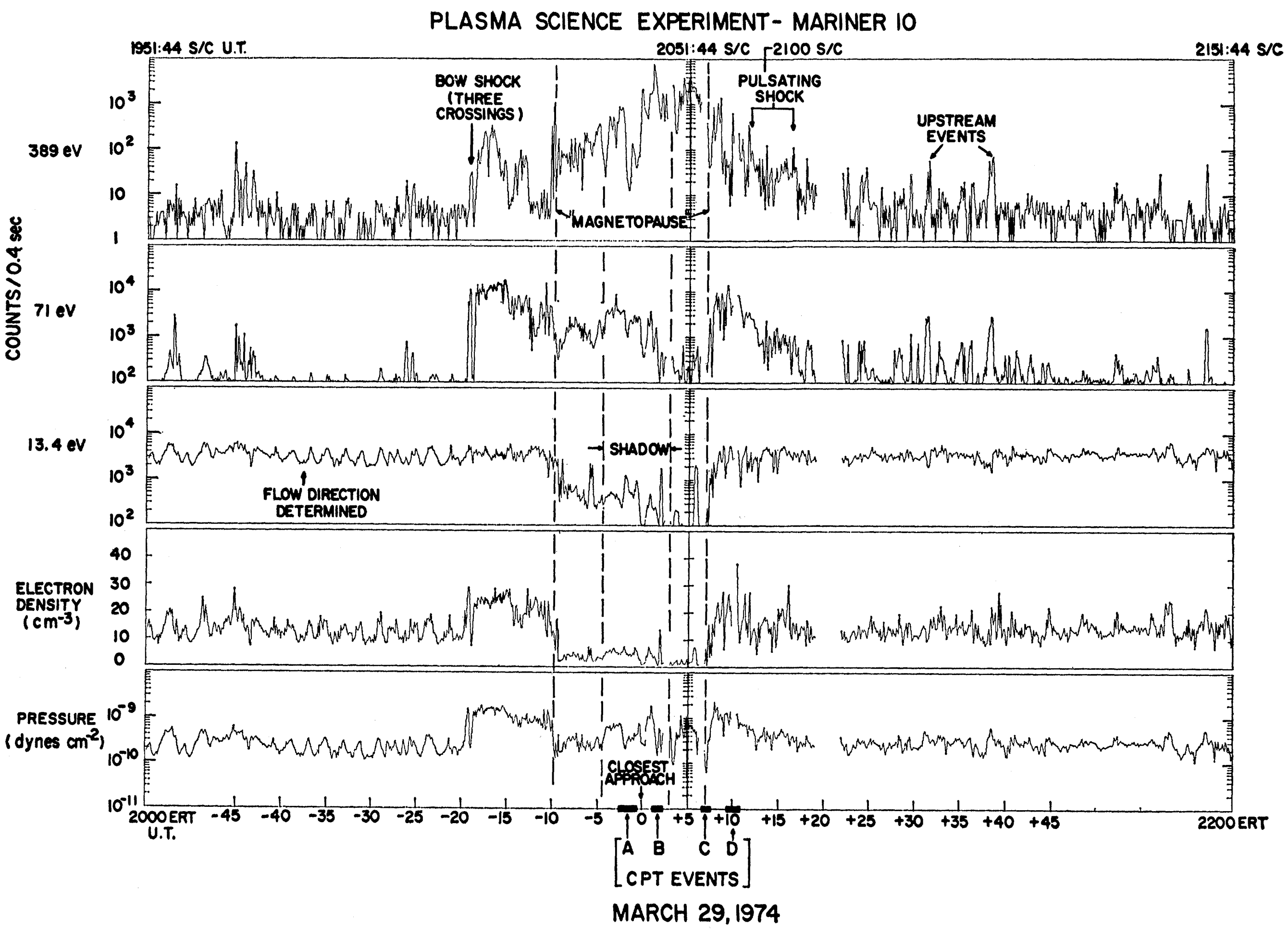

Fig. 3. Time plots of the fluxes observed at 389, 71, and 13.4 ev, and the density and pressure deduced from them. The times of events are indicated, and a time scale with zero at the time of closest approach is given along the bottom. The positions of the boundaries have been assigned on the basis of a consideration of the form of the electron spectrum; CPT, charged particle telescope experiment.

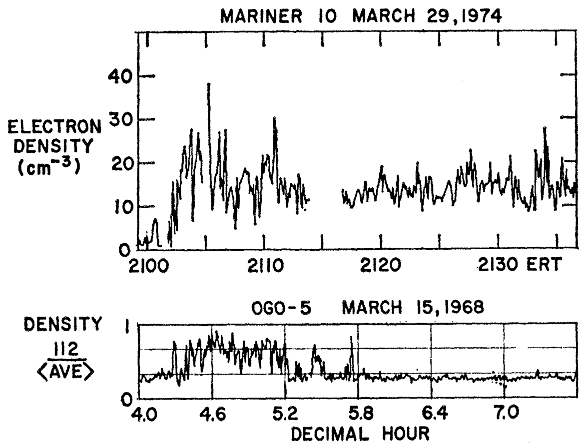

Fig. 4. Observations of a parallel shock made at Earth by OGO-5, compared with the present observations at Mercury. A scaling factor of $[c/(\omega_{pe} V_{sc})_{\text{Earth}}]/[c/(\omega_{pe} V_{sc})_{\text{Mercury}}]$ has been introduced to compensate for the different environments and spacecraft velocities, V_{sc}, when observing the two shocks. The ⟨112⟩ detector was "looking" toward the traversed shock, as was the Mariner 10 detector after pulsation (outbound) shock crossing.

sphere [as appears to be the case with Venus (*1*)]. The atmosphere of Mercury is thin or "exospheric"; that is, the mean free path for collisions is greater than the atmospheric scale height. The ultraviolet spectrometer experiment (*8*) gives an instrumental background upper limit on the column densities of 3×10^{13} cm^{-2} for neon, 10^{13} cm^{-2} for argon, a measured upper limit of 7×10^{11} cm^{-2} for helium and other column densities with lower values. In addition, an upper limit for the total pressure, P_T, at the terminator, to 2×10^{-9} mbar was inferred from the ultraviolet occultation experiment (*8*). To determine whether the atmosphere alone can stand off the solar wind, we consider the change in the velocity of the wind from its free streaming value, v, to its value v' after it has been slowed down by atmospheric mass addition at the rate $m_i J_i N_i$ (where m_i is the mass, J_i is the ionization rate, and N_i is the column density of the ith atmospheric constituent which behaves as a fluid). For this case, the one-dimensional continuity, momentum, and energy equations give

$$\frac{v}{v'} = \frac{\gamma}{\gamma - 1} \pm \left[\frac{1}{(\gamma - 1)^2} - \frac{\gamma + 1}{\gamma - 1} \sum_i \frac{m_i J_i N_i}{\rho v}\right]^{1/2}$$

where γ is the specific heat ratio and ρ is the solar wind mass density. This equation is consistent with the high-Mach number limit obtained previously (*9*). The plus sign corresponds to the formation of a shock; the minus sign refers to no shock. The maximum mass addition rate preceding the formation of a shock occurs when the argument of the square root vanishes. This fluid equation is realistic only when the ion gyroradius is smaller than the scale of the system, planet plus atmosphere. From the above, we find that the light constituents hydrogen and helium cannot stand off the solar wind. Since the gyroradii for heavier atmospheric ions, >12 atomic mass units, born in the solar wind, are of the order of the scale of the system, a microscopic point of view must be considered. In such cases the time it takes the solar wind to pass through a corresponding scale height is of the order of tenths of seconds while it takes much longer to accelerate heavy ions to the solar wind speed, of the order of tens of seconds for neon and argon. Hence, only a small impulse along the solar wind direction is imparted to heavy atmospheric ions as the wind passes through a scale height above the surface. On this basis we find that the momentum change of the solar wind along X_{sw} is negligible in traversing the maximum argon and neon atmosphere and seems to be small when passing through possible atmospheres limited by P_T. Consequently the solar wind, under this hypothesis, would be expected to strike the surface and be absorbed without forming a shock. However, the upper limits on the neutral gas would permit a strong limb shock (*10*). A limb shock seems to be excluded by the observed locations of the shock crossings, since they occur too far upstream. Therefore, we conclude that the solar wind must be deflected by a magnetic field.

The ionosphere within such a magnetic obstacle appears to be too weak to contribute appreciably to the total pressure. For this to occur a temperature > 10^5 °K would be required, based on the maximum possible ionospheric electron density of 10^3 cm^{-3} obtained from the radio occultation experiment (*11*). Such a temperature is untenably high.

The most likely source of the interaction at Mercury is thus a planetary magnetic field, either intrinsic or induced by the solar wind. It is instructive to consider the simplest possibility and to assume that the magnetic obstacle is a dipolar field. Using a theoretical model (*12*) for the locations of the terrestrial magnetopause and bow shock, we find the corresponding boundary crossings observed at Mercury can be fitted by varying the strength and location of a planetary dipole. In fitting to the model we assume that the dipole axis is perpendicular to the local orbital plane of the spacecraft, and that the Y_{sw}-Z_{sw} trace of the trajectory passes through the origin (Fig. 1). To a good approximation, this plane also contains the solar wind velocity vector, which is along $-X_{sw}$.

Figure 5 shows the result of such a scaling for three cases: case A, using the first inbound shock crossing, the two magnetopause crossings, and a solar wind flow 7° west of the sun; case B, using the last inbound shock crossing, the two magnetopause crossings, and a solar wind flow 7° west of the sun; and case B′, the same as case B but with the solar wind flow 3° west of the sun. For case A, we find that the distance from the center of the planet to the nose of the magnetopause is 1.6 R☿ and the dipole is located at $X_{sw} = 0.4$ R☿, $Y_{sw} = 0$, $Z_{sw} = 0$. Corresponding values for case B are as follows: nose distance = 1.25 R☿, dipole at $X_{sw} = 0.15$ R☿, $Y_{sw} = 0$, $Z_{sw} = 0$; for case B′ the values are: nose distance = 1.9 R☿, dipole at $X_{sw} = 0.55$ R☿, $Y_{sw} = 0$, $Z_{sw} = 0$. If we consider 0° flow, we find that the dipole must be located off the X_{sw} axis with a positive Y_{sw} coordinate. The fits give a range of dipole strengths from 4×10^{-4} to 9×10^{-4} times that of Earth. These dipole model fits clearly demonstrate the impossibility of a unique and accurate determination of the upstream stand-off distance of the magnetopause from the observations made during this single flyby, because of the sensitivity of this quantity to small variations in shock crossing times and flow direction. Furthermore, the dipole may be tilted in a direction different from that assumed, or it may be situated off the X_{sw} axis, or both. A preliminary estimate is that the present experiment can only determine the distance to the magnetopause nose to be less than 2.5 planetocentric radii.

In the above discussion we have not considered the origin of the magnetic field which causes the plasma interaction observed at Mercury. In general, there are three possible sources for the field: (i) an intrinsic planetary field; (ii) a steady-state induction process (unipolar generator); and (iii) an induction process arising from changes in the direction and magnitude of the incident magnetic field. Unfortunately, data from the present experiment do not allow an unambiguous choice from among these possibilities. Although the induction processes have been extensively discussed in the literature (*13*), a definitive three-dimensional model is still lacking. For any model which involves an induced magnetic field, some fraction of the incident plasma flow must contact the surface of the planet; hence in this case the nose of the "magnetopause" should coincide with the surface of the planet. Although, in principle, the position of the nose can be calculated from the measured boundary positions and from an adequate theory, as noted above, the measurements reported here lead to large uncertainties in the calculated positions even on the assumption that the theoretical models were complete. Given the experimental and theoretical uncertainties, no definite conclusions can be drawn concerning the origin of the magnetic field.

We consider next some detailed plasma features or events. The fluxes of electrons with energies greater than ~ 100 ev show interesting variations in the inbound magnetosheath, as illustrated by the 389-ev data field in Fig. 3. The flux increases by approximately a factor of 10^2 on crossing the shock and remains high for about 5 minutes. It then decreases to about twice the solar wind value for 1 minute, increases by a factor of 10 for 2 minutes, decreases to slightly greater than the solar wind value for 3 minutes, and remains low until the magnetopause crossing at −10 minutes. These variations might be temporal; however, the two intervals of decreased flux coincide with the times when the scanning angle of the instrument is directed toward the downstream shock (the instrument "looks" farthest from the planet), and the increased flux intervals coincide with scanning angles directed away from the downstream shock (the instrument "looks" closest to the planet). The variations, therefore, probably represent a directional asymmetry in the particle flux. This could be either a pressure or a streaming anisotropy directed downstream along draped field lines. The second possibility is more likely since the stronger upstream bow shock is a more intense source of electrons than the downstream bow shock.

A different scan modulation of the flux of the > 100-ev electrons was observed by the same instrument in the magnetosheath of Venus, where the highest fluxes were observed at scan directions farthest from the planet. A comparison of the two encounter geometries is given in Fig. 6 in which an inferred draped field line pattern, based on observed upstream magnetometer observations, is shown. In each case the ambient field had approximately the local corotation-spiral direction. At Mercury the maximum flux corresponds to electrons coming away from the upstream bow shock. A similar interpretation could be made for the anisotropy observed at Venus since the flux is a maximum when the instrument is viewing along a field line away from the planet and toward the point where the line crosses the bow shock. However, in the intervals of decreased flux at Venus, the fluxes were much less

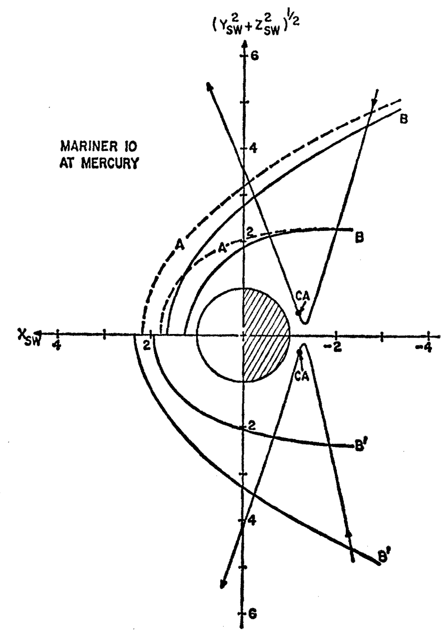

Fig. 5. (Top) The trajectory of Mariner 10, in a coordinate frame moving with the planet for the case of solar wind flow from a direction 7° west of the sun. This flow direction is that of the X_{sw} axis; *A–A* and *B–B* represent scaled magnetopause and bow shock boundaries, *A* for the incoming bow shock crossing occurring 1 minute before *B*; *CA* is the time of closest approach. (Bottom) *B′–B′*, the shock, and magnetopause corresponding to solar wind flow from a direction 3° west of the sun, and the same shock crossing time as *B*.

than the ambient solar wind fluxes, requiring an explanation in terms of an anisotropic electron removal rather than an anisotropic electron source. Figure 6 indicates that removal by interaction with the dayside atmosphere of Venus gives an explanation with the right asymmetery (*1*).

In the outbound magnetosheath of Mercury variations of the fluxes of energetic electrons also occurred, but these do not coincide with particular scan directions or with the scan period. They are interpreted as due to time-dependent generation by the pulsating shock encountered in the outbound interval. We note the absence at Mercury of intervals with energetic plasma electron fluxes less than ambient solar wind values such as occurred at Venus, and which we interpreted as atmospheric absorption. This absence of absorption is consistent with our earlier conclusion that the atmospheric interaction at Mercury is weak.

The changes in plasma properties observed in the Mercury magnetosphere could be either spatial features or temporal events. A single flyby does not permit a unique interpretation. The combination of highly structured plasma electron data, the magnetic field variations (*3*), and the energetic particle events observed in the magnetosphere suggest that a time-dependent interpretation is a reasonable possibility. If the magnetosphere is either induced or intrinsic, changes in the orientation of the external field can cause dramatic changes in structure. In the case of an induced field, this is obvious since the induced field must change as its driving electric field (equal to $-\bar{V}\times\bar{B}$ or $\partial\bar{B}/\partial t$) changes. For an intrinsic field (Earth's magnetosphere is the best-studied example), we know that rapid time changes occur during events known as substorms. There are some striking similarities between the Mercury observations interpreted as temporal events and substorm phenomenology in the magnetosphere of Earth.

To indicate that a substorm interpretation is a reasonable one to consider, we estimate the possibility of a substorm occurring in the 16 minutes Mariner 10 was in the Mercury magnetosphere, based on a scaling of the magnetosphere of Earth. The relevant time scale is the "convection time" given by the time to cycle all of the magnetic flux, F_t, in the tail under the action of the convection electric potential. The convection electric field varies from essentially zero when the interplanetary field is oriented antiparallel to the planetary dipole moment to a maximum when the interplanetary field is oriented parallel to the planetary dipole. The maximum potential is approximately $\phi_c = V_{sw}B_{sw}\ R_{☿}$, where V_{sw} and B_{sw} are the ambient solar wind speed and field strength and $R_{☿}$ is the scale size of the magnetosphere. If B_T is the field strength in the tail, the maximum convection electric field gives a minimum cycle time of

$$T_c = F_t/\phi_c \approx \frac{2\pi B_T R_{☿}}{B_{sw} V_{sw}}$$

For Earth a typical value of T_c is 60 minutes. Scaling to Mercury gives

$$(T_c)_{☿}/(T_c)_{\mathrm{Earth}} = (B_t\ R_{☿}/B_{sw})_{☿}\ (B_{sw}/B_t\ R_{☿})_{\mathrm{Earth}} \approx 1/50$$

That is, the convection time scale for Mercury is 1/50 that of Earth and is typically between 1 and 2 minutes. Thus, when the external field is oriented to give maximum convection, the substorm time scale for Mercury is approximately 1 or 2 minutes. If the plasma, field, and energetic particle events that began near -2 minutes are Mercury-variety substorms, they begin $\sim 4T_c$ before the spacecraft emerged from the magnetosphere. A consistent interpretation requires a change in external field orientation while the spacecraft was in the magnetosphere. This interpretation will be presented elsewhere (*14*).

The following conclusions may be drawn from the data presented here:

1) A fully developed bow shock and magnetosheath were observed near Mercury. These features provide unambiguous evidence for a strong interaction between Mercury and the solar wind.

2) Inside the magnetosheath there is a distinct region analogous to the magnetosphere or magnetotail of Earth. This region is populated by electrons with lower density and higher temperature than the electrons observed in the solar wind or magnetosheath.

3) The solar wind ram pressure, ρv^2, corresponds to a stagnation pressure equivalent to a magnetic field strength of 170 gammas.

4) The interaction is most likely not an atmospheric or ionospheric one. The assumption of an interaction with an intrinsic magnetic dipole requires a dipole strength approximately in the range 4×10^{-4} to 9×10^{-4} times that of Earth. The data do not preclude an

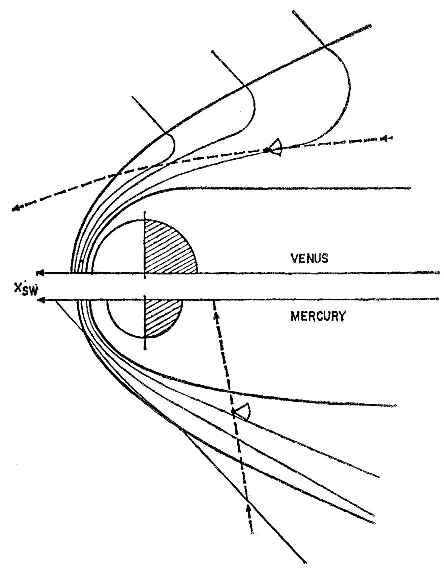

Fig. 6. A sketch of the trajectories of Mariner 10 (not to scale), in the vicinity of Venus and Mercury, and the directions of scanning of the instrument with respect to the likely magnetic field geometry.

interaction with an induced magnetic field.

5) The particle fluxes and the energy spectra show large variations while the spacecraft is inside the region we have called the magnetosphere. The variations could be either spatial or temporal in nature. It is possible that temporal events similar to substorms on Earth have been observed at Mercury.

6) At the time of observations, conditions were such that a perpendicular shock was observed on the inbound leg and a parallel shock was observed on the outbound leg of the trajectory. Energetic plasma electron events were observed upstream from the outbound shock crossing.

Appendix. In our analysis we have assumed that the spacecraft potential is negligible. In this section we discuss briefly the basis for that assumption and point out that there may have been some significant charging of the spacecraft during the period between events A and C.

If the spacecraft were charged positively, electrons would be accelerated toward the sensor and the peak of the electron distribution would be observed rather than the monotonically decreasing interplanetary spectra exemplified by spectrum 2 of Fig. 2 (*15*). Negative charging would move the distribution to lower energies but must be insignificant since both core and halo components were observed in the energy ranges observed for those components near Earth. In addition, the Mariner 10 densities scaled to 1 A.U. are in good agreement with near-Earth interplanetary densities measured by the LASL and MIT plasma experiments on Explorer 47 and Explorer 50.

During encounter, the possibility of charging to a negative potential can be tested by looking for changes in density when the spacecraft enters and leaves the shadow zone; no changes were observed. For the period beginning after energetic particle event A and ending with the magnetosheath reentry, there is a possibility that positive charging of the spacecraft occurred: the shape of spectrum 4 of Fig. 2 could be explained by a spacecraft potential near 50 volts, and the rather strange spectra observed between events B and C (when the counting rates were low at high and low energy but down to background levels for intermediate energies) could be due to a positive potential in the vicinity of a kilovolt. In that case, the high-energy channels would measure the low-energy portion of the shifted spectrum, and the low-energy counts, which are measured when the deflecting voltage is small, could be due to a large flux of higher energy particles striking a deflecting plate and producing spurious counts. We conclude that the only period of time in which spacecraft charging could have affected the measurements was between charged particle telescope (CPT) events A and C, and that during that time the spacecraft could only have charged positively, as noted above.

K. W. Ogilvie
J. D. Scudder
Laboratory for Extraterrestrial Physics, NASA Goddard Space Flight Center, Greenbelt, Maryland 20771
R. E. Hartle
Laboratory for Planetary Atmospheres, NASA Goddard Space Flight Center
G. L. Siscoe
Department of Meteorology, University of California, Los Angeles 90024
H. S. Bridge, A. J. Lazarus
Center for Space Research and *Department of Physics, Massachusetts Institute of Technology, Cambridge 02139*
J. R. Asbridge, S. J. Bame
University of California Los Alamos Scientific Laboratory, Los Alamos, New Mexico
C. M. Yeates
Jet Propulsion Laboratory, Pasadena, California 91109

References and Notes

H. S. Bridge, A. J. Lazarus, J. D. Scudder, K. W. Ogilvie, R. E. Hartle, J. R. Asbridge, S. J. Bame, W. C. Feldman, G. L. Siscoe, *Science* **183**, 1293 (1974).

M. D. Montgomery, J. R. Asbridge, S. J. Bame, *J. Geophys. Res.* **75**, 1217 (1970); J. D. Scudder, D. L. Lind, K. W. Ogilvie, *ibid.* **78**, 6535 (1973); W. C. Feldman, M. D. Montgomery, J. R. Asbridge, S. J. Bame, H. R. Lewis, paper presented at the 3rd Solar Wind Conference (Asilomar, Calif., 1974).

3. N. F. Ness, K. W. Behannon, R. P. Lepping, Y. C. Whang, K. H. Schatten, *Science* **185**, 151 (1974).
4. K. W. Ogilvie, J. D. Scudder, M. Sugiura, *J. Geophys. Res.* **76**, 3574 (1971); S. J. Bame, J. R. Asbridge, H. E. Felthauser, E. W. Hones, I. B. Strong, *ibid.* **72**, 113 (1967).
5. E. W. Greenstadt, I. M. Green, G. T. Inouye, D. S. Colburn, J. H. Binsack, E. F. Lyon, *Cosmic Electrodyn.* **1**, 160 (1970); E. W. Greenstadt, *J. Geophys. Res.* **77**, 1729 (1972); D. H. Fairfield, *ibid.* **74**, 3541 (1969).
6. K. A. Anderson, *J. Geophys. Res.* **74**, 95 (1969); F. L. Scarf, F. L. Fredricks, L. A. Frank, M. Neugebauer, *ibid.* **78**, 3697 (1973); W. C. Feldman, J. R. Asbridge, S. J. Bame, M. D. Montgomery, *ibid.* p. 3697.
7. J. A. Simpson, J. H. Eraker, J. E. Lamport, P. H. Walpole, *Science* **185**, 160 (1974).
8. A. L. Broadfoot *et al.*, *ibid.*, p. 166.
9. L. Bierman, B. Brosowski, H. Schmidt, *Solar Phys.* **1**, 254 (1967); P. A. Cloutier, M. B. McElroy, F. C. Michael, *J. Geophys. Res.* **74**, 6215 (1969); R. E. Hartle, S. J. Bauer, C. S. Wu, *Int. Assoc. Geophys. Aeron. Bull.* **34**, 569 (1973).
10. G. L. Siscoe and N. R. Mukherjee, *J. Geophys. Res.* **78**, 3961 (1973).
11. H. T. Howard *et al.*, *Science* **185**, 179 (1974).
12. J. R. Spreiter, A. L. Summers, A. W. Rizzi, *Planet. Space Sci.* **18**, 1281 (1970).
13. C. P. Sonett and D. S. Colburn, *Nature (Lond.)* **216**, 340 (1967); A. J. Dessler, in *Atmospheres of Venus and Mars*, J. C. Brandt and M. B. McElroy, Eds. (Gordon & Breach, London, 1968), pp. 241–250; F. S. Johnson and J. E. Midgley, *J. Geophys. Res.* **73**, 1523 (1968); J. V. Holweg, *ibid.*, p. 7269; G. Schubert *et al.*, *NASA Tech. Mem. X-62* (1973), p. 227.
14. G. L. Siscoe, K. W. Behannon, R. P. Lepping, N. F. Ness, *Geophys. Res. Lett.*, in press.
15. S. E. deForest, *J. Geophys. Res.* **77**, 651 (1972).
16. We thank all those whose work contributed to the success of the experiment and those whose names are listed in (*1*). We also thank members of the magnetometer, energetic particle, and ultraviolet teams on Mariner 10 for extensive discussions and comparisons of experimental results. We are grateful to E. W. Greenstadt for discussions concerning the nature of pulsating shocks, to V. Vasyliunas for discussions of spacecraft charging, and to M. Acuña for assistance in calibration, and to W. C. Feldman for helpful discussions.

29 May 1974

Magnetic Field Observations near Mercury: Preliminary Results from Mariner 10

Abstract. *Results are presented from a preliminary analysis of data obtained near Mercury on 29 March 1974 by the NASA-GSFC magnetic field experiment on Mariner 10. Rather unexpectedly, a very well-developed, detached bow shock wave, which develops as the super-Alfvénic solar wind interacts with the planet, has been observed. In addition, a magnetosphere-like region, with maximum field strength of 98 gammas at closest approach (704 kilometers altitude), has been observed, contained within boundaries similar to the terrestrial magnetopause. The obstacle deflecting the solar wind flow is global in size, but the origin of the enhanced magnetic field has not yet been uniquely established. The field may be intrinsic to the planet and distorted by interaction with the solar wind. It may also be associated with a complex induction process whereby the planetary interior-atmosphere-ionosphere interacts with the solar wind flow to generate the observed field by a dynamo action. The complete body of data favors the preliminary conclusion that Mercury has an intrinsic magnetic field. If this is correct, it represents a major scientific discovery in planetary magnetism and will have considerable impact on studies of the origin of the solar system.*

Results from a preliminary analysis of "quick-look" data obtained by the NASA-GSFC magnetic field experiment during Mercury encounter on 29 March 1974 are summarized in this report. The purpose of this investigation was to study the magnetic field environment of the planet Mercury and the nature of the solar wind interaction with it. There is substantial evidence in this initial assessment of the results to support the preliminary conclusion that an intrinsic planetary magnetic field exists. Rather unexpectedly, a very well-developed, strong, detached bow shock wave was observed, as well as a magnetosphere-like region in which the field magnitude increased to 98γ at closest approach, 704 km from the planetary surface. This is a factor of 5 greater than the average interplanetary magnetic field strength of 18γ measured outside the Mercurian bow shock.

Scientific interest in Mercury received a major stimulus in 1965 from data provided by radar observations of the planet. It was discovered (*1*) that the planet's rate of rotation was not synchronous with its orbital motion. Explanations for this remarkable result were soon forthcoming (*2*), and a new era in planetary studies began in which coupling of orbital motion and rotation rates was found to be considerably more complex and informative than previously expected.

For some time, it has been acknowledged that Mercury is anomalous among the terrestrial planets, having a remarkably high average density of 5.6 g/cm^3 for its small radius of 2434 km (*3*). Studies of the planet's interior have been hampered both by the inadequacy of available data concerning its shape, size, and mass and by the absence of definitive information concerning its rotational axis and precessional motion. Only recently have attempts been made to study these problems and their significance in the history of the formation of Mercury (*4*).

The atmosphere of Mercury has also been the subject of considerable speculation (*5*), the earlier work being prejudiced by the erroneous assumption of synchronous rotational and orbital periods. Studies incorporating new radar results (*6*) suggested that revision of the traditional concept of a planet devoid of an atmosphere was necessary.

In the absence of any evidence for appreciable rotation of the planet or for a substantial atmosphere, it was thought that Mercury would resemble our own moon in many respects. Taking into account recent observations of microwave emissions and the newly established correct rotation period for the planet, it was suggested strongly that its surface thermophysical characteristics would be rather close to those of the moon (*7*). There was no evidence for any radio emissions from Mercury such as those from Jupiter's radiation belts.

Thus, with the traditional view of geomagneticians that a rapidly rotating planet with some precession were features essential for generation of a planetary magnetic field (*8*), there was little reason to suggest an intrinsic field of Mercury. Some elementary estimates of a planetary magnetic field were made by using simple scaling laws for planetary volumes or rotation rates, or both, but the bases for these studies were rather speculative.

In specific studies related to the solar wind interaction with Mercury, the results depended on the planet's physical characteristics. Figure 1 summarizes four modes of interaction, of which three have been observed in the exploration of the solar system. In model A, a lunar type of interaction